The Journal of Korean Vacuum Science & Technology
Vol. 2, No. 2, October 1998, pp. 122~132

Silicon trench etching using inductively coupled Cl_2/O_2 and Cl_2/N_2 plasmas

Hyeon-Soo Kim, Young-Jun Lee and Geun-Young Yeom

Department of Materials Engineering, Sung Kyun Kwan University, Suwon 440-746, Korea
(Received March 4, 1998)

Abstract – Characteristics of inductively coupled Cl_2/O_2 and Cl_2/N_2 plasmas and their effects on the formation of submicron deep trench etching of single crystal silicon have been investigated using Langmuir probe, quadrupole mass spectrometer (QMS), X-ray photoelectron spectroscopy (XPS), and scanning electron microscopy (SEM). Also, when silicon is etched with oxygen added chlorine plasmas, etch products recombined with oxygen such as $SiCl_xO_y$ emerged and Si-O bondings were found on the etched silicon surface. However, when nitrogen is added to chlorine, no etch products recombined with nitrogen nor Si-N bondings were found on the etched silicon surface. When deep silicon trenches were etched, the characteristics of Cl_2/O_2 and Cl_2/N_2 plasmas changed the thickness of the sidewall residue (passivation layer) and the etch profile. Vertical deep submicron trench profiles having the aspect ratio higher than 5 could be obtained by controlling the thickness of the residue formed on the trench sidewall using Cl_2 (O_2/N_2) plasmas.

I. Introduction

Chlorine containing plasmas are widely used to etch various materials such as silicon, metal, III-V compound semiconductors, and GaN compound in the microelectronic device fabrication [1-3]. Diverse kinds of plasma sources including capacitively coupled plasmas [4-7] and high density plasmas sources such as electron cyclotron resonance plasmas (ECR) [8-10], helical resonator plasma (HR) [11-13], helicon plasma [14, 15], and inductively coupled plasma (ICP) [16-18] have been applied to the various types of silicon etching. Currently, various high density plasma sources are actively studied for semiconductor processing and most of the studies of silicon etching using high density plasmas are concentrated on the polysilicon etching of gate structures in semiconductor integrated circuits. Among the developed high density plasma sources, ICP has a benefit to generate large-diameter plasmas easily under a low pressure without magnetic field. Only a few publications using Cl_2 based high density plasmas by HR [12] or ECR [8-10] can be found for silicon trench etching that can be applied to the device isolation, trench capacitors, or microelectromechanical systems (MEMS) [9, 10, 18, 19].

Silicon etching processes including polysilicon etching and single crystalline silicon etching have been applied to semiconductor integrated circuit processing for many years. To etch silicon, chlorine, fluorine, or bromine based gases and their combinations have been used with additive gases such as oxygen or carbon containing gases to passivate the sidewall of etched silicon [1, 4, 11, 20]. In the pure chlorine plasmas for silicon etching, etched trench profiles often deviate from ideal sidewall profiles and the selectivity of silicon with respect to mask layer or photoresist is not often as high as desired. Therefore, most of the studies of the silicon etching use Cl_2, HBr, or fluorocarbon gas combination to passivate the sidewall of the etched silicon and hard mask like Ni and Cr are used in the deep silicon trench etching for MEMS application [9, 10].

The purpose of this work was to study the characteristics of inductively coupled chlorine based plasmas and their effects on the formation of submicron trench etching of single crystal silicon. This studies on the etching of the submicron single crystal silicon trenches using high density plasmas have never been reported except for shallow trench etching [18]. Compared to the conventional silicon etching, no cooling of the wafer and addition of bromine-containing gases such as HBr are utilized to obtain a vertical profile. As additive gases to chlorine plasmas, not only oxygen but also nitrogen were used to reduce the sidewall etching of silicon trenches. No researcher has been reported on the effects of Cl_2/N_2 high density plasmas on the silicon etching. In addition, one of the problems of the ICP etching, the degree of the quartz erosion was investigated and reduction methods was also considered in terms of process parameters.

II. Experimental Methods

To generate inductively coupled plasmas, 13.56 MHz rf inductive power was applied to a planar spiral coil (water cooled Cu coil, 3.5 turns) separated by a 1 cm-thick quartz window from the top of the process chamber after the introduction of process gas combinations. Separate 13.56 MHz rf power was also applied to the bottom electrode, where the substrate locates, to generate dc self bias voltages. Inductive power was varied from 200 to 800 Watts, and dc self-bias voltage from 0 to 80 volts. The dc-self bias voltage was measured using a high voltage probe (Tektronix P6015A).

A quadrupole mass spectrometer (QMS; Balzers QMG/E 125) located at the sidewall of the process chamber was used to monitor species such as dissociated radicals and etch products in the plasmas. Also, QMS was located on the chamber wall with 1 mm diameter-hole orifice and turbo-pumping system (2×10^{-6} Torr). A single Langmuir probe with 1.4 cm length and 0.03 cm diameter was also inserted into the center of the chamber to measure the ion densities of the plasmas. X-ray photoelectron spectroscopy (XPS; Fison Surface Systems ESCALAB 220i) has been used to estimate the residues remained on silicon trenches after the etching for different gas combinations and bias voltage conditions. Because it is difficult to separate the residue remained on sidewall of the silicon trench from that remained on the bottom of it, we analyzed the residues remained on the blank silicon wafers etched with and without dc bias voltage conditions. In addition, to investigate the source of excess oxygen found in our study, the erosion rates on of the quartz window located just below the inductive coil was estimated by measuring etch rates of thermal oxide located on the quartz window during the silicon etching.

To investigate the effects on silicon etch rates and selectivities over SiO_2 mask layer of the various process parameters such as inductive power, bias voltage, gas combination, etc., 1 μm-thick undoped polysilicon and 0.3 μm-thick oxide grown on silicon wafers were etched respectively under the same etch conditions. Etch rates and selectivities were estimated using a Nanospec by measuring the thickness of the films before and after the etching. To etch deep silicon trenches, 0.3 μm-thick thermal oxide grown on p-type silicon wafers were patterned with a photomask and etched to make submicron openings from 0.25 to 0.8 μm. The patterned thermal oxide was used as the mask layer after removing the photoresist. After silicon trench etching, scanning electron microscope (SEM) was used to observe the etch rate, etch selectivities, and profiles of the submicron silicon trenches.

III. Results and Discussion

A. Plasma diagnostics of Inductively coupled Cl_2/O_2 and Cl_2/N_2 plasmas

Characteristics of the plasmas measured by plasma diagnostic tools such as mass spectrometer, optical emission spectroscope, Langmuir probe, etc. can be used to explain the dependency of etch rate and selectivity on process variables, and can be also helpful for the understanding of the change of etch profile of silicon trench [21]. In this study, a single Langmuir probe and a quadrupole mass spectrometer have been used to characterize the chlorine based inductively coupled plasmas. The Langmuir probe was biased up to −40 volts whose saturated values gives the ion densities [16]. Fig. 1 shows the measured ion current densities as a function of inductive power for different gas combinations of 100% Cl_2, Cl_2+ 5%~15%O_2, and Cl_2+5%~15%N_2 at the constant total pressure of 5 mTorr. As the inductive power increased, the ion current density increased almost linearly, however, the addition of oxygen or nitrogen to chlorine reduced the ion current densities. Also, the addition of nitrogen showed the higher ion current densities compared to that of oxygen for the same percentage of the additives. Even though ionization energy for nitrogen is the highest among oxygen (13.6 eV), nitrogen (14.5 eV), and chlorine (12.9 eV), lowest ion current densities for the oxygen contained chlorine plasmas appear to be related to the higher electronegativity of oxygen compared to nitrogen. When ion current densities were measured for Ar plasmas for the same conditions, about 45% higher ion current densities were obtained compared to that of the chlorine plasmas. The ion densities of Ar plasmas were in the range of $2\sim5\times10^{11}/cm^3$.

Fig. 2 shows the effects of inductive power on the chlorine radical densities measured by QMS for the same conditions as Fig. 1. Increase of

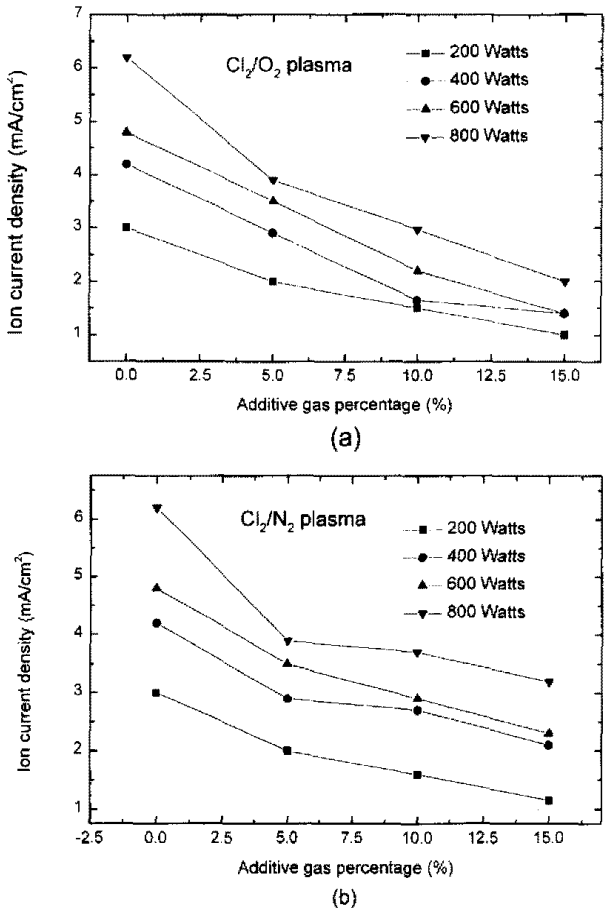

Fig. 1. Ion current densities measured by a Langmuir probe as a function of additive gas percentage and inductive power for (a) Cl_2/O_2 and (b) Cl_2/N_2 plasmas at 5 mTorr. The Langmuir probe was biased at -40 volts and located at the center of the chamber to estimate ion densities of the plasmas.

inductive power increased radical densities, however, oxygen added chlorine plasmas also showed the lowest chlorine radical densities. The chlorine radical density was reduced not only by the reduction of chlorine gas density at the same pressure by the addition of oxygen but also by the recombination of chlorine radicals with oxygen atoms in the plasma. From the QMS analysis for the inductive power over 600 W, the mass peak corresponding to Cl_2O was observed even though it is not the same species such as ClO_x - reported by other researchers while operating oxygen contained chlorine plasmas [5, 19, 22]. In case of nitrogen added chlorine plasmas, no such recombined species were found and only

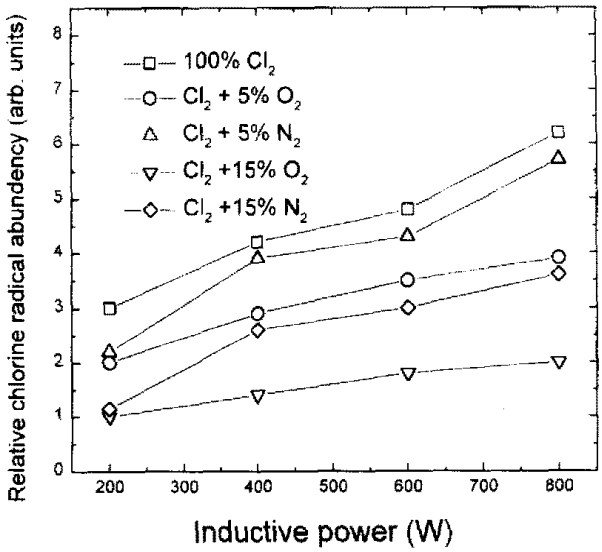

Fig. 2. Relative chlorine radical intensity as functions of inductive power and plasma chemistries as the same conditions of Fig. 1.

feed gases and their radicals were observed.

B. Surface interaction between plasmas and silicon

While the silicon etching process was monitored by QMS. Other species related to silicon etch byproducts were also observed. Fig. 3 shows that main etch products were $SiCl_x$ (x=2, 3, 4) and the most abundant species was $SiCl_3$ or $SiCl_4$ depending on process conditions. As the inductive power increased, the $SiCl_x$ etch products decreased, and it is probably due to the increased redissociation of the etch products at higher inductive power conditions [10, 12]. In addition, as the bias voltage increased at a constant inductive power of 600 Watts and pure chlorine plasmas, main etch products change from $SiCl_3$ to $SiCl_4$ due to the increase of incident chlorine radical. The effects of the addition of oxygen or nitrogen to chlorine on etch products observed by the mass spectrometer while silicon is etched are shown in Table 1. As oxygen is added to chlorine plasmas, new etch products such as $SiCl_xO_y$ are observed in accordance with other researcher's results [4, 5, 11, 19, 22] and, at the same time, the

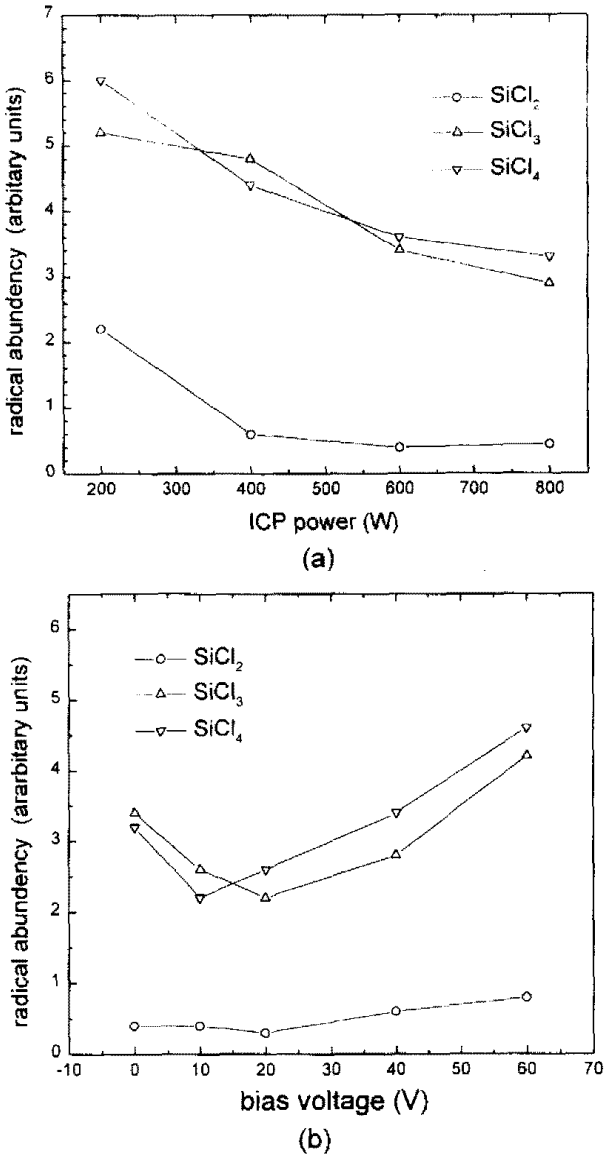

Fig. 3. SiClx radical intensity as functions of (a) inductive power and (b) bias voltage in the 100% Cl_2 plasmas.

total amounts of $SiCl_xO_y$ such as $SiCl_2O$, $SiClO_3$, and $SiClO_2$ within the mass range limit (200 amu) increased with the increase of added oxygen percentages. Also, $SiCl_2$ became the most abundant etch product while other main radicals such as Cl, $SiCl_3$, and $SiCl_4$ are reduced. When silicon is etched in nitrogen added chlorine plasmas, nitrogen radical itself was observed and no other etch products recombined with nitrogen radical were observed, and the plasmas were similar to the 100% chlorine plasmas as shown in Table 1.

Fig. 4 shows Si 2p narrow scan XPS data for

Table 1. The effects of oxygen or nitrogen addition to chlorine plasmas on the radicals or etch products observed by a quadrupole mass spectrometer while silicon is etched at 600 Watts of the inductive power and −40 volts of the dc self bias voltage. (10^{-8} mbar of the partial pressure of reactive gase).

	Cl	$SiCl_2$	$SiCl_3$	$SiCl_4$	$SiCl_2O$	$SiClO_3$	$SiClO_2$
100%Cl_2	30	0.5	2.3	3.3	–	–	–
Cl_2/5%N_2	22	0.8	2.7	2.8	–	–	–
Cl_2/10%N_2	17.5	0.25	1.7	1.6	–	–	–
Cl_2/5%O_2	20	0.7	1.1	1.9	0.5	–	0.2
Cl_2/10%O_2	14.5	2.4	1.5	1.4	1.9	0.6	0.2
Cl_2/15%O_2	10	2.2	1.6	1.6	1.5	1.7	0.6
Cl_2/30%O_2	6.5	1.2	0.6	0.4	1.3	0.9	0.4

silicon surfaces etched in Cl_2(a), Cl_2/15%O_2(b), or Cl_2/15%N_2(c) plasmas with and without −40 volts of applied dc self bias voltage. Differences of the residue composition with and without bias voltages (or ion bombardment energy) can be related to the chemical states of the silicon surfaces at the bottom and the sidewall of the silicon trenches, respectively. Fig. 4(a) shows peaks near 99.5 eV and 102.5 eV that correspond to Si-Si bonding and possibly Si-Cl-O bonding, respectively. Si-Si and Si-Cl-O bond peaks measured for silicon etched with −40 volts of dc bias voltage are similar to those for silicon without dc bias voltage for the pure Cl_2 case. The atomic ratio of Si:Cl:O on the silicon surface etched with −40 volts dc bias voltage was 61:7.5:31.5. In case of silicon etched by oxygen added chlorine plasmas without applied dc bias voltage show another peak at 103.5 eV corresponding to Si-O bonding. The peak area of Si-O bonding increased with the increase of oxygen percentage in the plasmas (not shown). However, silicon etched with −40 volts of dc bias voltage in the 10% oxygen added plasma did not show the peak corresponding to Si-O bonding and the silicon 2p peak shape was similar to that of 100% chlorine. This result is considered due to the reduction of the residue layer by enhanced ion bombardment. The increase of oxygen percent in chlorine plasma at a fixed −40 volts of dc bias voltage increased oxygen atomic percent in Si-Cl-O bonding of the etched silicon surface and with 30% of oxygen in chlorine plasmas, a peak corresponding to Si-O bonding showed up even with −40 volts of dc bias voltage. The atomic ratios of Si : Cl : O for 15% and 30% oxygen with −40 volts of dc bias voltage were 53.3 : 7.2 : 39.5 and 29.2 : 1.2 : 69.6, respectively. In case of silicon etched by nitrogen added chlorine plasmas, no peaks were found corresponding to Si-N, and peak shapes were similar to those of 100% chlorine plasmas and there were no significant differences in peak areas found in the XPS data of silicon surface etched with and without applied bias voltage.

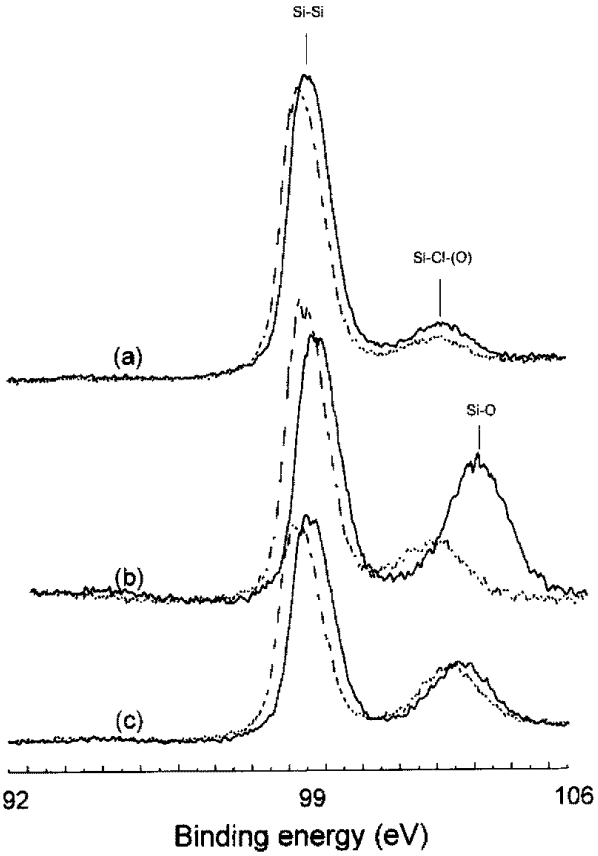

Fig. 4. Silicon 2p narrow scan data measured by X-ray photoelectron spectroscopy on the silicon surfaces etched by (a) Cl_2, (b) Cl_2/15%O_2, and (c) Cl_2/15%N_2 plasma with (– – – – –) and without (————) −40 volts of applied dc self bias voltage.

C. Quartz erosion during silicon etching

Oxygen found on the silicon etched in 100% chlorine plasmas or nitrogen added chlorine plasmas is possibly not only from the exposure to air before the XPS analysis but also from the quartz window erosion during the silicon etching. Currently, studies on quartz erosion have been reported by other researchers for HR for silicon etching [14] or ICP during oxide etching [23]. This quartz erosions are confirmed by some methods as follows in this experiments. When 400 Watts of rf power is applied to the center of the coil while the outside of the coil is grounded, about 1 kV of zero-to-peak rf voltage measured by a high voltage probe is induced at the center of the coil and from this voltage, therefore, a certain voltage is induced between the plasma and the center of the quartz window. When 100% chlorine or Cl_2/N_2 plasmas were generated, oxygen radicals possibly originated from the erosion of the quartz window were observed. Therefore, to estimate the erosion of the quartz window, small sizes of thermal oxide wafers were taped on the center of the quartz window where the rf induced voltage was highest and the erosion rates of thermal oxide were measured. It turned out that the thermal oxide wafers were eroded at different etch rates depending on plasma conditions. In 100% chlorine plasmas, as the rf inductive power increased or bias voltage decreased, the thermal oxide erosion rate increased. As shown in Fig. 5, for 600 Watts of inductive power, thermal oxide was eroded with 320 Å/min at −20 volts of applied dc bias voltage and 140 Å/min at −60 volts. The addition of nitrogen from 0 to 15% did not change the erosion rates of thermal oxide, and the erosion rates were similar to the pure chlorine cases. However, the addition of oxygen to chlorine plasmas drastically reduced thermal oxide erosion rates, and when more than 10% oxygen was added, the erosion rate decreased to less than 50 Å/min.

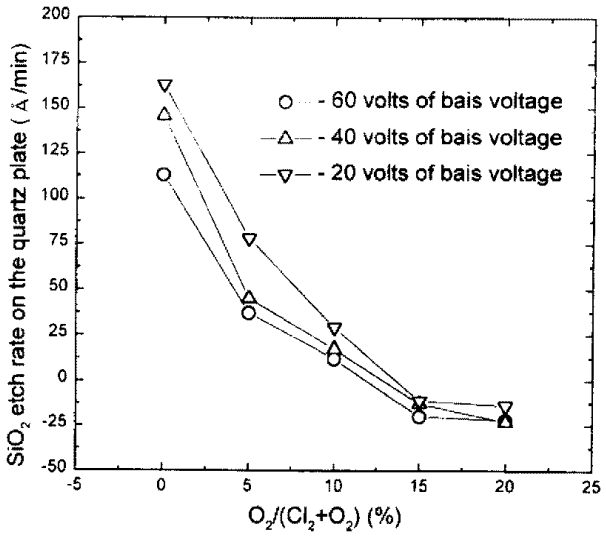

Fig. 5. The quartz erosion rates measured by etch rate of thermal oxide on the quartz plate as a function of gas combination of Cl_2 and O_2 and dc bias voltage at 600 Watts of inductive power.

Therefore, in our experimental conditions, the presence of oxygen on the etched silicon wafers is inevitable even though no oxygen was added to the feed gas combinations. In addition, conventional effects of small amounts of additive oxygen gas (under 10%) on the change of silicon etch rate were not investigated in this experiments in contrast to the other ICP data. Polysilicon etch rate continuously decreased with the small oxygen addition from 0 to 10%. Effects of Faraday shield on the erosion rates of quartz window are currently under investigation to find a way to reduce the erosion rate [23].

D. Silicon etch rate and etch selectivity over oxide mask

Polysilicon etch rates increased with the increase of inductive power, however, the etch selectivity over oxide mask decreased in all of the plasma chemistry. For example, polysilicon etch rates increased from 800 Å/min to 2500 Å/min as the inductive power increased from 200 to 800 Watts in the 100% Cl_2 plasmas and bias voltage of −40 volts. The maximum etch selectivity over oxide mask, easily formed by conventional

thermal oxidation unlike metal hard mask [8-10], could be obtained by lowering the bias voltages. However, the decrease of the bias voltage resulted in lower silicon etch rate and etch-stop in the high oxygen addition (> 25%). In the Cl_2/O_2 plasmas, silicon etch rates with sufficient ion energy (bias voltage) because high energy ion bombardments are needed to break the nonvolatile Si-O bonds on the silicon surface. Optimized bias voltage showing the maximum selectivity to thermal oxide mask increased with the increase of the oxygen addition. In the Cl_2/N_2 plasmas, silicon etch rates are similar to that of the pure Cl_2 plasmas but etch selectivity decreased with increase the of the nitrogen addition due to the oxide etching enhancement. From these basic etch characteristics of polysilicon and silicon oxide, optimum process conditions could be selected for the silicon trench etching.

The effects of the additive gases on the average etch rates of the silicon trenches having trench widths from 0.3 to 0.8 μm and the etch selectivities over thermal oxide mask layer are shown in Fig. 6 for 600 Watts of inductive power and −40 volts of dc self bias voltage. As shown in the figure, as oxygen or nitrogen is added to chlorine, the silicon etch rates decreased due to the reduction of chlorine ions and radicals available for silicon etching as shown in Figs. 1 and 2, however, decreased at much faster rates for oxygen added chlorine plasmas compared to the nitrogen added chlorine plasmas, which is possibly due to the decrease of chlorine ions and radicals for oxygen added plasmas as shown in Figs. 1 and 2, and also possibly due to the recombination of oxygen with silicon as shown in XPS data of Fig. 4. The etch rates of the thermal oxide were also decreased with the addition of oxygen or nitrogen, and the etch rates for the oxygen added plasmas were much smaller than those for nitrogen added plasmas. Therefore, silicon etch selectivities over thermal oxide were

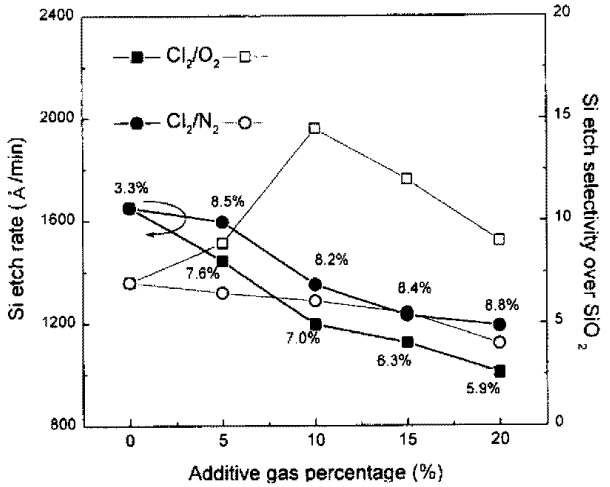

Fig. 6. The silicon etch rates (solid) and etch selectivities (open) over thermal oxide mask layer etched using Cl_2, Cl_2/O_2, and Cl_2/N_2 plasmas at 600 Watts of the inductive power and −40 volts of dc self bias voltage. This etch rates are average etch rates for the various trench widths from 0.25 to 0.8 μm and the number (%) written in the figure shows the dependence of the silicon trench etch rates on the trench widths.

higher for the oxygen added chlorine plasmas. When nitrogen was added, the etch selectivity decreased linearly with the increase of nitrogen addition, however, when the oxygen was added, the etch selectivity showed a maximum in the range of oxygen percentage of 10~15% and it is probably related to the formation of Si-O bonding on silicon surface at above a certain oxygen percentage under a fixed bias voltage as described above. Undoped polysilicon etch rates were similar to the etch rates of 0.8 μm silicon trenches, however, there appeared to be some dependence of silicon trench etch rates on the trench widths as written in numbers (%) in Fig. 6. [6, 9]. Smaller trench widths showed lower silicon etch rates and as nitrogen or oxygen was added, its effect became larger. However, as the dc self bias voltage increased, the difference became smaller (not shown).

E. Etch profiles of submicron silicon trenches

Etched silicon trenches were observed using SEM and the effects of additive gases on sub-

micron trench profiles are shown in Fig. 7 for the silicon trenches etched at 600 Watts of inductive power and −40 volts of dc self bias voltage in 100%Cl_2(a), Cl_2/5%O_2(b), Cl_2/15%O_2(c), or Cl_2/10%N_2(d). Submicron silicon trench etching with pure chlorine (a) showed some degree of sidewall etching during the deep trench etching due to no sidewall passivation as observed in Fig. 4(a). However, as 5% oxygen was added, the trench profile improved as shown in Fig. 7(b) due to the sidewall passivation as shown in Fig. 4(b). However, the small addition of oxygen was not enough to protect the exposed sidewall of the trenches when deep trenches were etched, therefore, higher percentage of oxygen had to be added to protect the sidewall of the trenches by forming a sidewall passivation layer [14, 24]. The sidewall passivation layer was composed of Si-Cl-O and Si-O bonding possibly from the etch products as observed by the mass spectrometer in Table 1. This sidewall passivation layers could be easily removed by 10 : 1 HF dipping in contrast

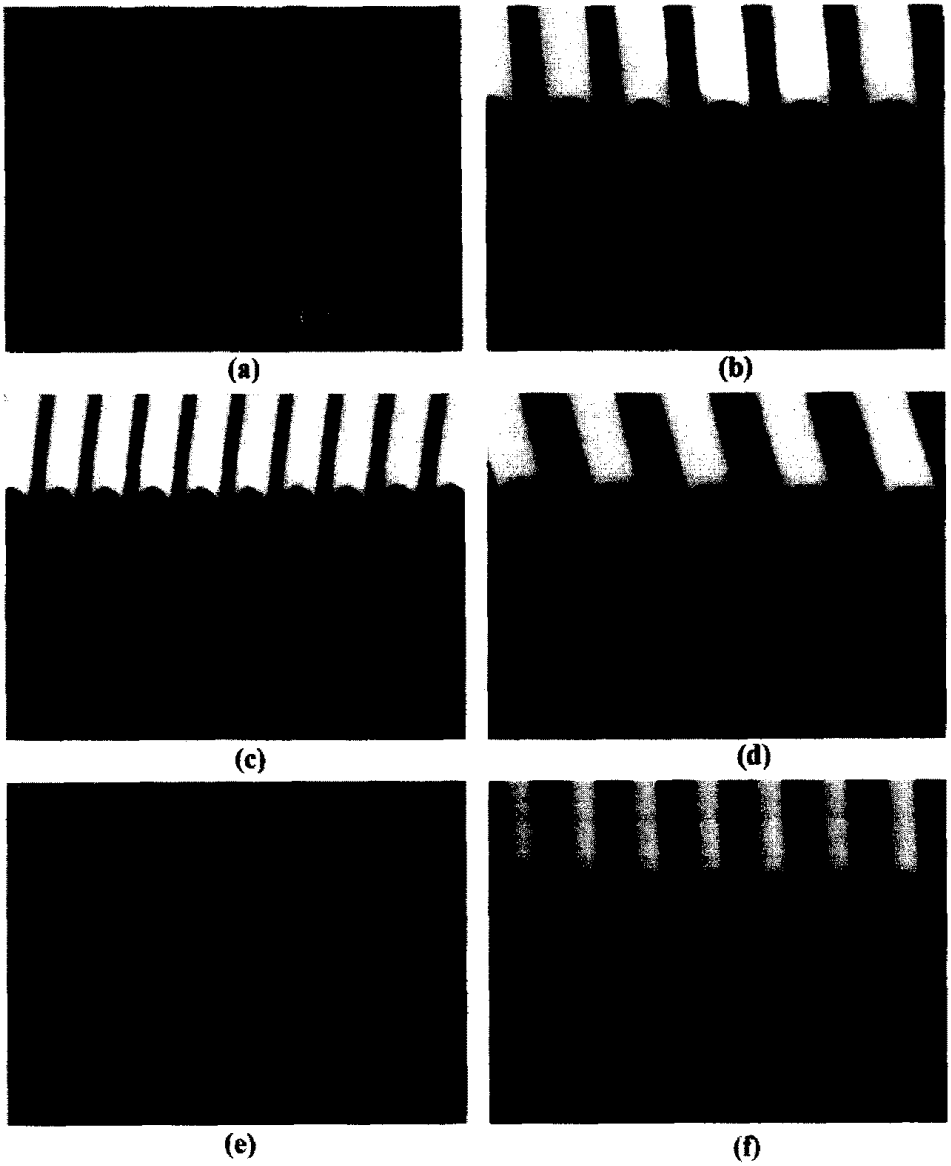

Fig. 7. SEM micrographs of the submicron silicon deep trenches etched by (a) Cl_2, (b) Cl_2/5% O_2, (c) Cl_2/15%O_2, (d) Cl_2/10%N_2, and (e) Cl_2/10%O_2/5%N_2 plasmas at 600 Watts of inductive power and −40 volts of dc self bias voltage and (f) Cl_2/15%O_2 plasma at 400 Watts of inductive power and −80 volts of dc self bias voltage.

to C-F polymer on the etched silicon surface in the contact oxide etching or silicon etching using fluorocarbon gas as a main etch gas or additive gas to halogen gases. This is probably an adequate method for the silicon trench etching of micron sizes, however, when deep submicron trenches are etched as shown in Fig. 7(c), the sidewall passivation layer formed on the top area of the submicron trench tends to narrow the trench width and vertical trench etching becomes impossible as the trench etch depth is increased due to the closing of the trenches and due to the scattering of incident ions by the sidewall passivation layer [24].

Fig. 7(d) shows the effect of nitrogen addition on the silicon deep trench profile. The addition of nitrogen to chlorine was also effective in reducing the sidewall etching. As seen in Fig. 3 and Table 1, no etch products related to nitrogen recombination were found in nitrogen added chlorine plasmas and no Si-N bonding were found on the etched silicon surface. Therefore, it is believed that there is no such a sidewall passivation mechanism that happens for oxygen added chlorine plasmas when silicon is etched with nitrogen added chlorine plasmas. Instead, in nitrogen added chlorine plasmas, the lack of chlorine radical on the sidewall due to the nitrogen addition possibly reduced the etch rates of the sidewall compared to the those of the trench bottom, therefore, vertical trench shapes could be obtained. This results could be supported by some etch experiment using Cl_2/Ne plasmas. The silicon trenches etched by Cl_2/Ne plasmas at 600 Watts of inductive power and -40 volts of dc self bias voltage were observed using SEM and showed similar profiles to the Cl_2/N_2 plasmas. On the other hands, though we tried to observe the sidewall and bottom of the submicron trench by XPS analysis, we could not completely distinguish which may suggest that the chemical competition of the chemical states of the sidewall from those of the bottom in the silicon trenches etched by various conditions. Sidewall becomes similar to those of the oxide mask as the trench width narrows.

Oxygen and nitrogen were added together to chlorine to reduce the thickness of sidewall passivation layer and to obtain more anisotropic etch profiles, and one of the etch profiles for the oxygen and nitrogen added chlorine plasmas is shown in Fig. 7(e). Near vertical deep trenches with a thin sidewall passivation layer could also be obtained with 15% oxygen by increasing the dc self bias voltage as shown in Fig. 7(f) for silicon trenches etched in 15% oxygen added chlorine plasmas at -80 volts of dc self bias voltage. Increasing dc bias voltage increases trench etch rates compared to sidewall etch rates, reduces time to form a thicker sidewall passivation layer, and also can reduce sidewall residue by energetic ion bombardment even though it reduces etch selectivity. Fig. 7(f) shows a vertical submicron silicon trench profile for 0.3 μm-width trench having 6 : 1 aspect ratio. As a result, submicron silicon trenches having high a aspect ratio could be obtained by optimizing process conditions such as gas combinations, bias voltage, etc. However, some problems still remain in the submicron silicon trench etching including mask erosion subjected to energetic ion bombardments into oxide mask and ion scattering due to the operation pressure at 5 mTorr.

IV. Conclusions

Characteristics of inductively coupled chlorine-based plasmas (Cl_2, Cl_2/N_2, and Cl_2/O_2) and their effects on the formation of submicron deep trench of single crystal silicon were investigated. Compared to the conventional etch results, no cooling of the wafer and addition of bromine-containing gases such as HBr are necessary to obtain a vertical profile and no polymer depositions are

used for sidewall passivation.

Ion current density measured by a Langmuir probe and Cl radical density observed by QMS decreased with the addition of nitrogen or oxygen, however, the addition of oxygen to chlorine reduced the ion current density and the Cl radical density more significantly compared to the nitrogen addition by the recombination of oxygen with chlorine. When silicon is etched, oxygen in chlorine plasmas also changed the main etch products to $SiCl_2$ from $SiCl_3$ or $SiCl_4$ for pure chlorine plasma and other etch products recombined with oxygen such as $SiCl_xO_y$ emerged. However, nitrogen in chlorine plasmas did neither recombine with chlorine nor recombine with any of the etch products. XPS analysis of the silicon surfaces etched with or without bias voltage in nitrogen or oxygen added chlorine plasmas showed that silicon surfaces etched with or without bias voltage in Cl_2/N_2 plasma are similar each other, while the silicon surfaces etched in Cl_2/O_2 plasmas are not. A peak related Si-O bonding corresponding to a passivation layer was found without bias voltage for oxygen added chlorine plasmas. Quartz window erosion was investigated by measuring the antenna voltage and etch rate of thermal oxide piece glued to the window. The erosion rate reduced with the addition of oxygen increase of bias voltage. When silicon trenches were etched, the characteristics of Cl_2/N_2 and Cl_2/O_2 plasmas changed the thickness of sidewall residue and trench profiles. Thick sidewall residues were formed for the oxygen added chlorine plasmas especially at higher oxygen percentage, while no thick sidewall residues were found for nitrogen added chlorine plasmas. Near vertical deep submicron (0.3 μm) trench profiles having the aspect ratio higher than 5 could be obtained by controlling the residue thickness formed on the trench sidewall using Cl_2/N_2, Cl_2/O_2 and $Cl_2/O_2/N_2$ plasmas.

References

1. D. M. Manos and D. L. Flamm, *Plasma Etching: An Introduction* (Academic, 1989), p. 146.
2. S. J. Pearton, C. B. Vartuli, R. J. Shul and J. C. Zolper, Material Sci. and Eng. **B31**, 309 (1995).
3. J. Hong, J. W. Lee, E. S. Lambers, C. R. Abernthathy, C. J. Santana, S. J. Pearton, W. S. Hobson, and F. Ren, J. of Electronic Materials **25**, 1428 (1996).
4. S. C. McNevin, J. Vac. Sci. Technol. **A9**, 816 (1991).
5. N. Ozawa, T. Matsui, and J. Kannamori, Jpn. J. Appl. Phys. **34**, 6815 (1995).
6. D. Chin, S. H. Dhong, and G. J. Long, J. Electrochem. Soc. **132**, 1705 (1985).
7. H. Crazzolara and N. Gellrich, J. Electrochem. Soc. **137**, 708 (1990).
8. K. T. Sung and S. W. Pang, J. Vac. Sci. Technol. **A11**, 214 (1993).
9. W. H. Juan and S. W. Pang, J. Vac. Sci. Technol. **A14**, 1189 (1996).
10. W. H. Juan and S. W. Pang, J. Vac. Sci. Technol. **A13**, 834 (1995).
11. K. V. Guinn, C. C. Cheng, and V. M. Donnelly, J. Vac. Sci. Technol. **B13**, 214 (1995).
12. I. P. Herman, V. M. Donnelly, C. C. Cheng, and K. V. Guinn, Jpn. J. Appl. Phys. **35**, 2410 (1996).
13. C. C. Cheng, K. V. Guinn, and V. M. Donnelly, J. Vac. Sci. Technol. **B14**, 85 (1996).
14. F. H. Bell, O. Joubert, and L. Vallier, J. Vac. Sci. Technol. **B14**, 1796 (1996).
15. F. H. Bell, O. Joubert, and L. Vallier, J. Vac. Sci. Technol. **B14**, 96 (1996).
16. J. B. Carter, J. P. Holland, E. Peltzer, B. Richardson, E. Bogle, H. T. Nguyen, Y. Melaku, D. Gates, and M. Ben-Dor, J. Vac. Sci. Technol. **A11**, 1301 (1993).
17. R. Patrick, P. Schoenborn, H. Toda, and F. Bose, J. Vac. Sci. Technol. **A11**, 1296 (1993).
18. G. Zhao, T. Ko, J. D. Chinn, J. Electrochem. Soc. Spring, Abstract p. 286 (1996).
19. M. Sato and Y. Arita, J. Electrochem. Soc. **134**, 2856 (1987).
20. K. Nishikawa, T. Oomori, K. Ono, and M. Tuda, Jpn. J. Appl. Phys. **35**, 2421 (1995).
21. O. Auciello and D. L. Flamm, *Plasma Diasgnostics vol. 1* (Academic, 1989).

22. J. H. Thomas III and L. H. Hammer, J. Appl. Phys. **68**, 2400 (1990).
23. Y. Hikosaka, M. Nakamura, and H. Sugai, Jpn. J. Appl. Phys. **33**, 2157 (1994).
24. G. S. Oehrlein, J. F. Rembetski, and E. H. Payne, J. Vac. Sci. Technol. **B8**, 1199 (1990).
25. J. C. Arnold, D. C. Gray, and H. H. Swain, J. Vac. Sci. Technol. **B11**, 2071 (1993).